Development of a novel deformation-amplified shape memory alloy-friction damper for mitigation of seismic effects on buildings

Kaiming Bi[1], Zhenhua Zhang[2] and Hong Hao[3]

1. Senior Lecturer, Centre for Infrastructure Monitoring and Protection, School of Civil and Mechanical Engineering, Curtin University, Bentley, WA 6102, Australia. Email: kaiming.bi@curtin.edu.au

2. School of Civil Engineering, Henan Polytechnic University, Jiaozuo 454000, P. R. China. Email: zhangzh@hpu.edu.cn

3. John Curtin Distinguished Professor, Centre for Infrastructure Monitoring and Protection, School of Civil and Mechanical Engineering, Curtin University, Bentley, WA 6102, Australia. Email: hong.hao@curtin.edu.au

Abstract

Shape memory alloys (SMAs) have been widely used to mitigate seismic responses of engineering structures due to its good self-centring capability. However, the energy dissipation capacity of SMA-based dampers are generally limited compared to other dampers due to the narrow hysteretic loops. To improve the energy dissipation capacity, a novel deformation-amplified SMA-friction damper (DASMAFD) is proposed in the present study. In this damper, the displacement from the structure is amplified by a lever mechanism in the damper, so that the self-centring and energy dissipation capacities of the damper can be better used as compared to the one without amplification. Experimental tests demonstrated the good performance of this damper.

Keywords: DASMAFD; SMAs; friction damper; experimental study.

1. Introduction

Shape memory alloy (SMA) is a good candidate to make self-centring dampers due to its unique shape memory ability under heating or unloading [1]. Moreover, SMA dampers exhibit stable energy dissipation capability, which makes them able to dissipate certain amount of energy during earthquake excitation, such that the more important structural components are protected. Due to these advantages, extensive research works have been carried out, and a variety of SMA-based dampers [2-8] have been proposed and investigated since 1990's. Almost all these studies showed that the SMA-based devices are effective in mitigating the seismic responses and reducing the residual deformations of engineering structures.

However, it should be noted that, compared to other traditional dampers such as the friction dampers, viscous dampers and BRBs, the energy dissipation capacity of SMA-based dampers are relatively limited because of its flag-shaped hysteretic behaviour. On the other hand, it is well known that the damping capacity of a damper is strongly related to the relative response (displacement, velocity or acceleration) between the two ends of the device, and increasing the sensitivity of the damper to the relative response

is helpful to enhance the damping effectiveness. Recently, some deformation amplification dampers have been proposed and investigated [9-14]. These studies showed that dampers with displacement amplification mechanism show improved seismic control effectiveness compared to the ones without amplification.

In the present study, a novel deformation-amplified SMA–friction damper (DASMAFD) is proposed. This novel damper consists of a deformation-amplified SMA system and a friction element in parallel. In particular, a lever system is employed to amplify the deformation transferring from the structure to the SMA wires, and a friction adjusting system is adopted to adjust the friction force in the damper. This novel system thus can take advantages of the excellent self-centering capability of superelasticity of SMA and the prominent damping capacity of the friction element. To examine the performance of this novel system for seismic induced vibration control, the design and mechanism of the device are presented in detail, and the self-centering and damping capacity of the damper are investigated through experimental studies.

2. Damper development

The DASMAFD is composed of a deformation-amplified SMA system (DASMAS) and two friction adjusting systems (FASs) in parallel, and its 2D and 3D structural sketches are shown in Figure 1. As shown, the DASMAS is composed of four SMA wires, eight sliding slots, four sliding rods, four swing plates, four fixed pins, two transfer bars, two baseboards and one actuator lever. The two upper sliding rods connected by SMA wires can move along the two upper sliding slots, and the original working length of SMA wires is determined by the distance between the two sliding rods as shown in Figure 1(a). The swing plates are installed onto the baseboard through the fixed pins, and they can rotate around the fixed pins. Each swing plate contacts with the corresponding sliding rod initially as shown in Figure 1, and the other end connects with the transfer bar installed on the moving actuator lever (refer to the local 3D view in Figure 1(a)). When the actuator lever has relative movement with respect to the baseboard, it will drive the swing plates to rotate around the fixed pin through the transfer bar. In particular, when the actuator moves to the right, all the upper swing plates will rotate anticlockwise. The top left swing plate drives the left sliding rod moving along the left sliding slot, but the right sliding rod is restrained by the left end of the right sliding slot. On the other hand, if the actuator moves to the left, the movements of the above mentioned parts will be reversed. Therefore, whether the actuator lever moves to the left or right, the distance of the two sliding rods will increase, which induces tensile deformation to the SMA wires connecting by the two sliding rods, hence more energy dissipation.

The two FASs are shown in Figure 1(b). As shown, each FAS is made of a support, an adjusting screw, a group of disc-springs, and a guiding pad. The support is fixed onto the baseboard by two bolts. The support has a through-hole, the upper part of which is threaded while the lower part is not. Meanwhile, a hole with the same size as the through-hole is drilled in the baseboard under the hole in the support with a depth of half of the baseboard's thickness, and the remaining half is excavated into a rectangle shape to host the rectangular head of the guiding pad. The guideway of the guiding pad (i.e. the lower part of the guiding pad) is matched with the actuator lever, so that the guiding pad can move along the actuator lever. Then the disc-springs are inserted into the holes of support and baseboard on the top of the head of the guiding pad, and the adjusting screw is tightened into the threaded hole to supply compressive force to the disc-springs and thus the pressure to the contact surface between the guiding pad and actuator lever. When the actuator lever has a movement relative to the baseboard, friction force will be induced at the contact surface, and this friction force can be

adjusted by the adjusting screw. With the above designs, a DASMAFD was manufactured, and Figure 2 shows the front and top views of a DASMAFD sample.

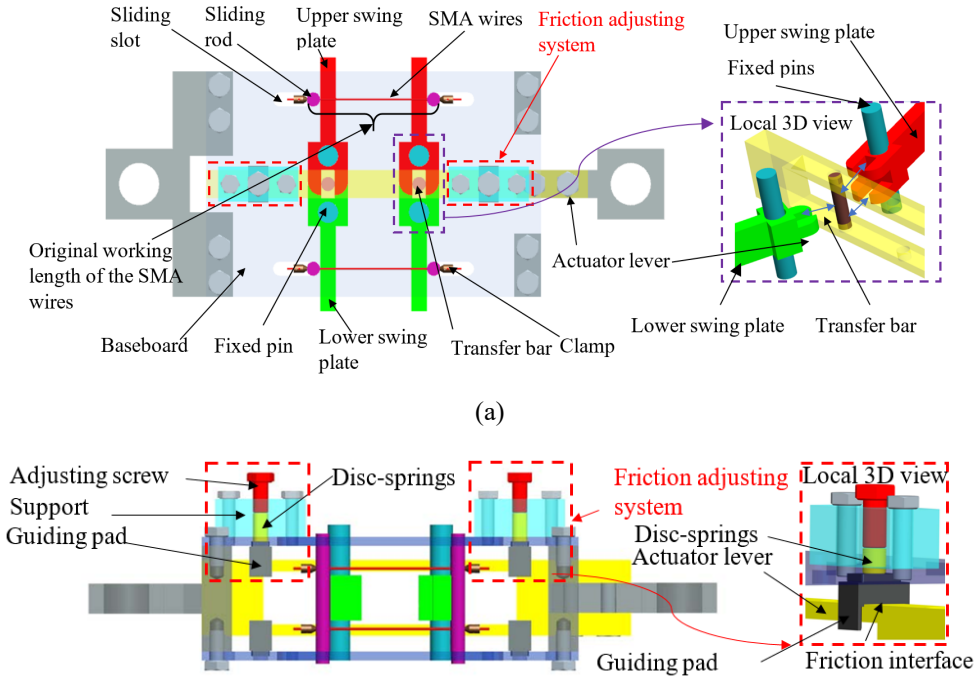

Figure 1. 2D and 3D sketches of the DASMAFD: (a) front view, (b) top view, (c) 3D view

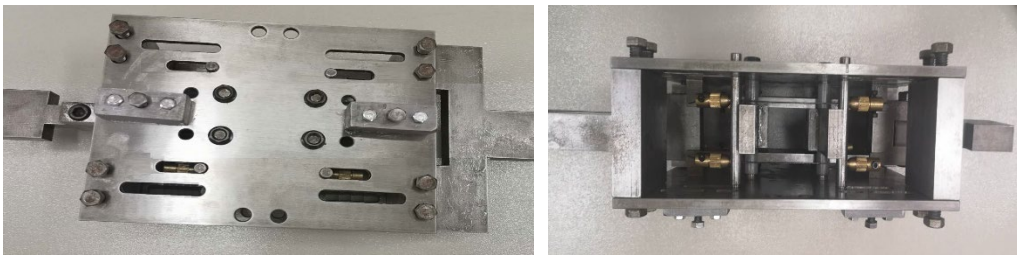

(a) (b)

Figure 2. Photos of the prototype DASMAFD device: (a) front view, (b) top view.

3. Working mechanism

When the proposed damper is used to control the vibration of a frame structure subjected to the earthquake loading, it can be installed onto the structure by fixing the two ends to adjacent floors in each storey of the frame as shown in Figure 3. The working mechanism of the DASMAFD has been briefly introduced in the above section, and it is further explicitly illustrated in Figure 4. As shown in Figure 4(a), when the damper is under tension, the actuator lever will introduce a relative displacement δ to

the right, the upper swing plates will rotate around the fixed pins anticlockwise, and the SMA wires connecting to the two sliding rods will be extended with a tensile deformation Δ. Similarly, the same deformation will apply to the SMA wires when the damper is subjected to the compressive deformation (see Figure 4(c)). According to the geometry as shown in Figure 4, the ratio between Δ and δ, which is defined as the deformation amplification ratio (DAR), has the following relationship:

$$\varphi = \frac{\Delta}{\delta} = \frac{h_2}{h_1} \tag{1}$$

where h_1 is the vertical distance between the fixed pin and the transfer bar, and h_2 is the corresponding distance between the sliding rod and the fixed pin.

It is obvious that φ has the following three scenarios:

Case 1, $\varphi < 1$: the deformation of the SMA wires (Δ) is smaller than the input deformation (δ) induced by the inter-storey drift of the structure. In this case, the deformation is actually de-amplified by the damper.

Case 2, $\varphi = 1$: the deformation of the SMA wires is equal to the input deformation. In this case, the damper behaves the same as a normal shape memory alloy-friction damper (SMAFD), where the deformation is not amplified.

Case 3, $\varphi > 1$: the deformation of the SMA wires is larger than the input deformation, i.e., the interstorey drift, the deformation from the structure is amplified.

To enhance the vibration control effectiveness, Case 3 is considered in the present study. For comparison, Case 2 is also discussed. In the present study, only one DASMAFD was manufactured, and the different DARs were achieved by adjusting the distance between the sliding rod and the fixed pin (i.e. h_2). As shown in Figure 2(a), eight sliding slots were drilled in the baseboard. When the SMA wires were installed between the inner four slots, $\varphi = 1$ was achieved, when the SMA wires were installed between the outer four slots, φ equals to 2, namely the displacement from the structure will be amplified by two times.

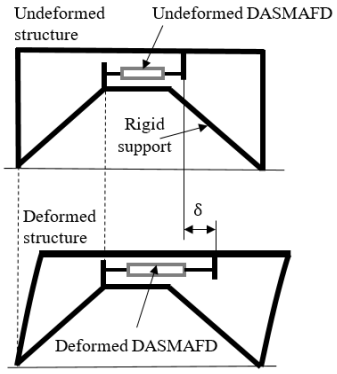

Figure 3. The installation and deformation of the DASMAFD

To conveniently quantify the energy dissipation capabilities of the damper, it is convenient to define the following relationship:

$$F_{\mathrm{f}} = mF_{\mathrm{Ms}} \tag{2}$$

where F_{f} is the friction force between the guiding pad and the actuator lever, and F_{Ms} is the martensitic transformation starting force of the SMA wires which is shown in Figure 5, and m is the ratio between F_{f} and F_{Ms}, which can be dubbed friction proportion (FP).

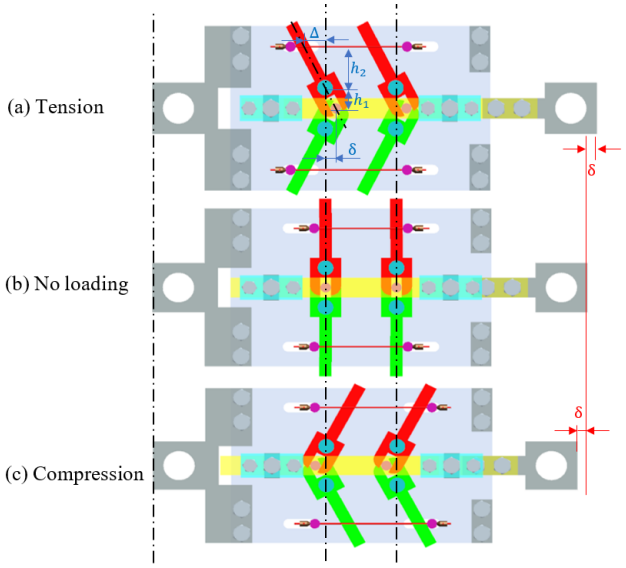

Figure 4. Working mechanism of the damper

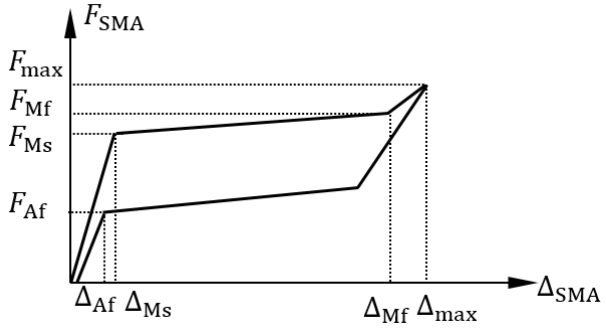

Figure 5. Schematic force-deformation relationship of the SMA wires.

4. Experimental study and mechanical property of the damper

After the development of the damper, its mechanical property was tested by using a universal testing machine (EUTM). Figure 6 shows the testing setup. As discussed above, two scenarios were considered in the present study, i.e. with $\varphi = 1$ (SMAFD) and $\varphi = 2$ (DASMAFD) respectively by adjusting the SMA wires position at different sliding slots (refer to Figure 2). For the FP, five cases with m=0, 0.25, 0.5, 0.75 and 1 respectively were tested, and the different FPs were achieved by changing the force of the adjusting screw.

Figure 6. Mechanical property test of the DASMAFD

The hysteretic curves of the SMAFD and DASMAFD under different FPs are shown in Figure 7. The x-axis of the figure is the relative displacement between the two ends of

the damper (δ), and a maximum value of 4 mm was tested. The maximum extension of the SMA wires in the SMAFD was 4 mm since φ = 1, while that in the DASMAFD was 8 mm because φ was set to be 2. Figure 7(a) shows the results when *m*=0. In this case, no friction force was applied to the damper, and both dampers were equivalent to the conventional SMA damper but with different maximum extensions. It can be seen that both dampers showed excellent self-centering capability, and they almost went back to their original positions after unloading. Moreover, both dampers showed stable energy dissipation capabilities. These results are actually expected since both dampers became the conventional SMA damper as mentioned above, the self-centering and energy dissipation capacities were controlled by the SMA wires only, which should follow the stress-strain behaviour of the SMA wires as shown in Figure 5. The results also show that the force in the DASMAFD was larger than that in the SMAFD, this is because the force provided by the damper is related to the DAR φ, and larger φ results in larger force. When friction force was added (Figures 7(b) to (c)), it can be seen that the hysteresis loop became fuller and F_D became larger with the increment of FP, which indicates the friction system enhanced the energy dissipation capacity of the dampers. On the other hand, the results also show that with the increase of FP, larger residual displacements were observed for the both dampers, and this effect was more evident in SMAFD. As shown, when FP reached 1.0 (Figure 7(c)), SMAFD lost its self-centering capability. This is because the recovering force from SMA wires was resisted by the friction force, hence SMA wire could not recover to its original position. For the DASMAFD, though the residual displacement also increased with the increment of FP, it showed much better self-centering capability compared to the SMAFD. As shown in Figure 7(c), very small residual displacement were obtained even though the FP reached 1. This is because the lever arm from the SMA wires is longer than the friction force. Although the force in SMA wires is the same as the friction force, the arm length of the SMA wires to the pin is longer, therefore inducing a larger moment which overcomes that from the friction force, and leads to recovery of the deformation. The results clearly demonstrate the advantages of DASMAFD compared to SMAFD.

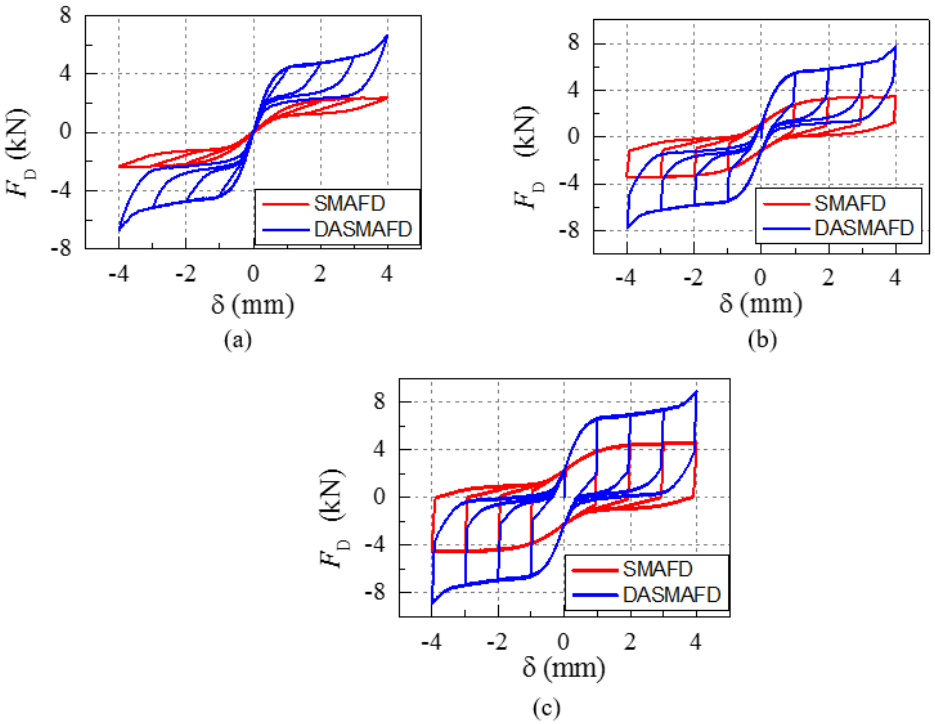

Figure 7. The influence of FP on the force-displacement relationship of different dampers, (a) *m*=0, (b) *m*=0.5, and (c) *m*=1

5. Conclusions

A novel deformation-amplified SMA–friction damper (DASMAFD) is proposed in the present study. The design, mechanism of the damper are introduced and experimental studies are carried out to examine the mechanical behaviour of the damper. Experimental results show that the damper has better self-centering and energy dissipation capacities compared to the one without displacement amplification.

References

[1] Cisse C, Zaki W, Zineb T B. A review of constitutive models and modeling techniques for shape memory alloys. International Journal of Plasticity, 2016, 76: 244-284.
[2] Zuo XB, Li AQ. Numerical and experimental investigation on cable vibration mitigation using shape memory alloy damper. Structural Control and Health Monitoring, 2011, 18(1): 20-39.
[3] Parulekar Y M, Kiran A R, Reddy G R, Singh R K, Vaze K K. Shake table tests and analytical simulations of a steel structure with shape memory alloy dampers. Smart Materials and Structures, 2014, 23(12): 125002.
[4] Qian H, Li H N, Song GB, Guo W. Recentering shape memory alloy passive damper for structural vibration control. Mathematical Problems in Engineering, 2013, 2013: 963530
[5] Qiu CX, Zhu S Y. Shake table test and numerical study of self-centering steel frame with SMA braces. Earthquake Engineering & Structural Dynamics, 2017, 46(1): 117-137.
[6] Zhou P, Liu M, Li H, Song GB. Experimental investigations on seismic control of cable-stayed bridges using shape memory alloy self-centering dampers. Structural Control and Health Monitoring, 2018, 25(7): e2180.
[7] Fugazza d. Use of shape-memory alloy devices in earthquake engineering: mechanical properties, advanced constirutive modelling and structural applications. PhD thesis 2005; Universita degli Studi di Pavia.
[8] Morais J, Gil de Morais P, Santos C, Campos Costa A, Candeias P. Shape memory alloy based dampers for earthquake response mitigation. 2nd International Conference on on Structural Integrity, 4-7 September 2017, Funchal, Portugal.
[8] Ribakov Y, Reinhorn A M. Design of amplified structural damping using optimal considerations. Journal of Structural Engineering, 2003, 129(10): 1422-1427.
[9] Huang CH. Parametric study for motion amplification device with viscous damper. 13th World Conference on Earthquake Engineering. Vancouver Canada, 2004.
[10] Li H, Mao CX, Ou JP. Experimental and theoretical study on two types of shape memory alloy devices. Earthquake Engineering & Structural Dynamics, 2008, 37(3): 407-426.
[11] Walsh KK, Cronin KJ, Rambo-Roddenberry MD, Grupenhof K. Modeling and simulation of an amplified structural damping system in a seismically-excited truss tower. Active and Passive Smart Structures and Integrated Systems 2010. International Society for Optics and Photonics, 2010, 7643: 76432S.
[12] Londoño JM, Neild S A, Wagg DJ. Using a damper amplification factor to increase energy dissipation in structures. Engineering Structures, 2015, 84: 162-171.
[13] Baquero Mosquera JS, Almazán JL, Tapia NF. Amplification system for concentrated and distributed energy dissipation devices. Earthquake Engineering & Structural Dynamics, 2016, 45(6): 935-956.